RSC Advances

This is an *Accepted Manuscript*, which has been through the Royal Society of Chemistry peer review process and has been accepted for publication.

Accepted Manuscripts are published online shortly after acceptance, before technical editing, formatting and proof reading. Using this free service, authors can make their results available to the community, in citable form, before we publish the edited article. This *Accepted Manuscript* will be replaced by the edited, formatted and paginated article as soon as this is available.

You can find more information about *Accepted Manuscripts* in the Information for Authors.

Please note that technical editing may introduce minor changes to the text and/or graphics, which may alter content. The journal's standard Terms & Conditions and the Ethical guidelines still apply. In no event shall the Royal Society of Chemistry be held responsible for any errors or omissions in this *Accepted Manuscript* or any consequences arising from the use of any information it contains.

ROYAL SOCIETY OF CHEMISTRY

www.rsc.org/advances

Please do not adjust margins

Journal Name

ARTICLE

Novel Organic Memory Effect from Donor-Acceptor Polymers based on 7-Perfluorophenyl-6*H*-[1,2,5]thiadiazole[3,4-g]benzoimidazole

Received 00th January 20xx,
Accepted 00th January 20xx

DOI: 10.1039/x0xx00000x

www.rsc.org/

Benlin Hu, [a] Chengyuan Wang,[a] Jing Zhang,[a] Kai Qian, [a] Pooi See Lee,[a] Qichun Zhang*[ab]

A novel D-A conjugated polymer (PIBT-BDT) with 7-perfluorophenyl-6*H*-[1,2,5]thiadiazole[3,4-*g*]benzoimidazole has been synthesized through the Stille coupling reaction. The memory device with PIBT-BDT as an active layer shows a large on/OFF ratio (> 10^5), good endurance (> 100 cycles), and long retention (>10^4 s). Through simulating the *I-V* curves and analysing energy barriers in the device structure, we suggest that the memory effect of Au/PIBT-BDT/ITO is originated from the charge transfer between the strong acceptor (IBT) units and the donor BDT units.

Introduction

Over the last 50 years, resistive switching, referring to the physical phenomena where a dielectric sharply changes its resistance under the effect of a strong electric field or current, has attracted numerous attentions for its charmingly potential application in memories, logic calculation and artificially neuromorphic synapses.[1-8] Especially, the resistance memory, i.e. resistance random access memory (RRAM), has advantages of simple structure, mass storage, high operation speed, and being compatible with traditional CMOS technology.[9-15] Since the Ag/$Pr_{0.7}Ca_{0.3}MO_3$(PCMO)/$YBa_2Cu_2O_{7-x}$(YBCO) sandwiched structure was firstly explored as RRAM,[16] a large number of inorganic and organic materials have been explored as RRAM materials, such as complex oxides, binary oxides, amorphous silicon, organic small molecules, conjugated polymers, functional polyimides, chromophores pendent polymers and polymer nanocomposites (blended with carbon nanomaterials and metal nanoparticles).[17-33] Compared with inorganic materials and most organic small molecules,[4,6,25] polymers show more interests in the application as RRAM due to their unique characteristics of high scalability, highly tailorable, easy solution processability, flexibility, high mechanical strength and three-dimensional stacking capability.[17,19,22,25]

Donor-acceptor polymers based on 2,1,3-benzothiadiazole (BT) have been widely explored as optic-electrical materials, such as organic field-effect transistor (OFET), organic photovoltaic device (OPV) and organic light-emitting diode (OLED).[34-39] However, less effort about D-A polymers based on BT units was reported with memory effect. Moreover, because the electron-withdrawing ability of the BT unit is not strong enough, BT units as acceptors in polymers usually need to further be modified by other electron-withdraw groups. The fluorination for polymers has received numerous attentions in materials science due to the interesting improvements of the properties of materials by introducing fluorine atoms into the structure, such as better solubility, high oxidative stability and degradation resistance.[40-43] Especially, conjugated fluoropolymers used in organic electronics have been reported to possess lower LUMO energy levels, better electrode interface to the injection of charge carriers, and high stability to the ambient species (O_2/H_2O) since the fluorine atom is the most electronegative element. In fact, conjugated fluoroligomers and conjugated fluoropolymers have been demonstrated to show excellent performances in OFETs, OPVs and OLEDs .[34-37,39]

In this contribution, a new D-A conjugated polymer (**PIBT-BDT**, see **scheme 1**) based on novel acceptor with a strong electron-deficient pentafluorophenyl group, 7-perfluorophenyl-6*H*-[1,2,5]thiadiazole[3,4-*g*]benzoimidazole (**IBT**), incorporated into the BT unit to enhance the electron-withdrawing ability has been designed and synthesized. The as-synthesized polymer has high molecular weight (M_n) of 14 Ka by means of gel permeation chromatography (GPC) analysis against a linear polystyrene standard. The polymer is readily soluble in common organic solvents, such as toluene, chloroform, tetrahydrofuran and chlorobenzene. The sandwiched device of Au/ **PIBT-BDT** /ITO shows an excellent nonvolatile memory effect, such as high ON/OFF ratio, good endurance and long retention. The memory effect is derived from the charge transfer between of **IBT** units and BDT units.

EXPERIMENTAL

Materials and methods

4,7-Dibromo-5,6-diaminobenzothiadiazole[44] (**4**) and **M2**[39,45] (Scheme 1) were prepared according to the reported procedures. All starting chemicals, unless otherwise specified, were purchased from Alfa Aesar or Sigma-Aldrich and used as received.

[a] School of Materials Science and Engineering, Nanyang Technological University, Singapore 639798, Singapore. Email: qczhang@ntu.edu.sg.
[b] Division of Chemistry and Biological Chemistry, School of Physical and Mathematical Sciences, Nanyang Technological University, Singapore 637371, Singapore

RSC Advances Accepted Manuscript

Please do not adjust margins

Journal Name

ARTICLE

Scheme 1. The synthesis of the monomer (M1) and the polymer (PIBT-BDT)

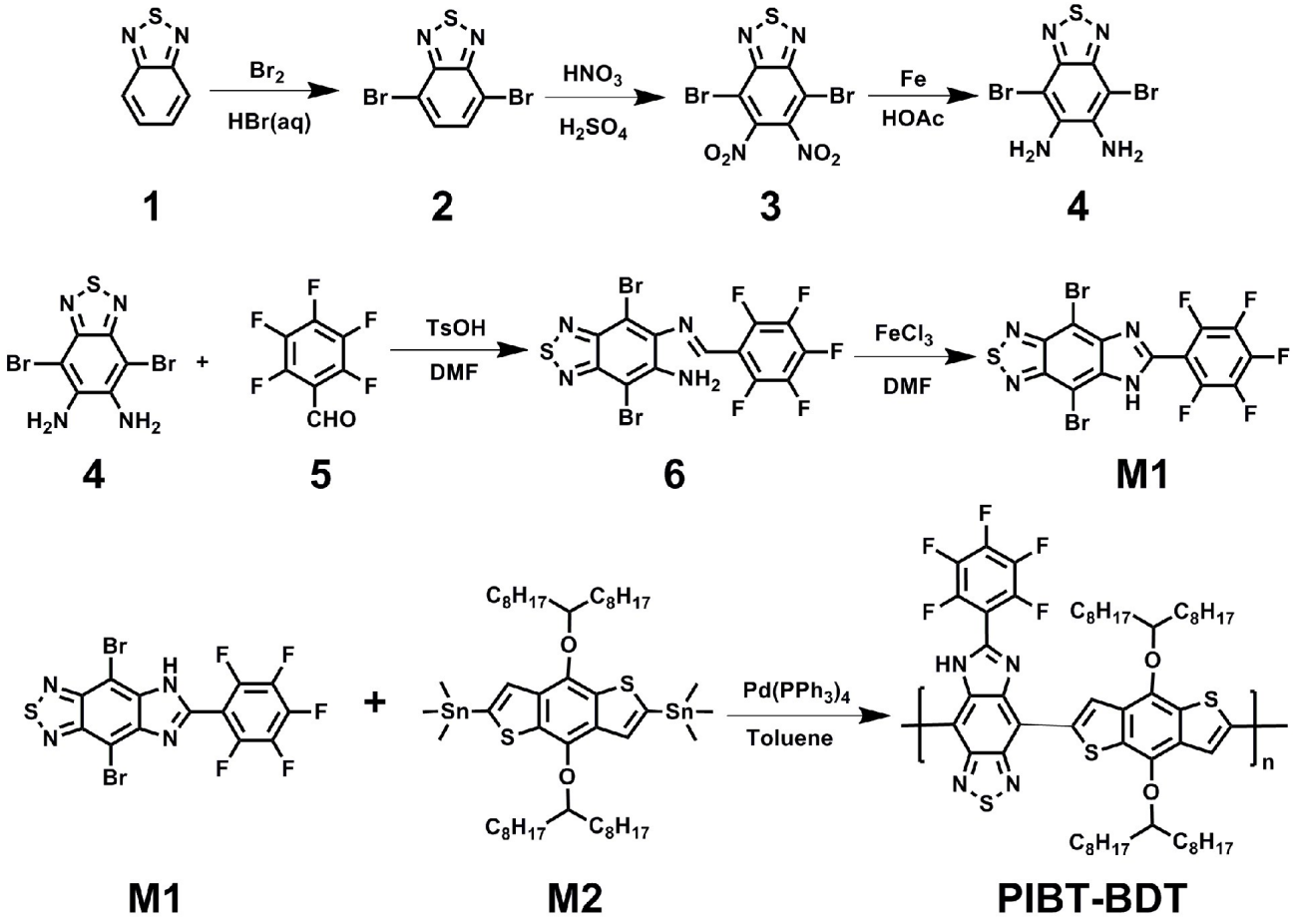

^{1}H Nuclear Magnetic Resonance (^{1}H NMR) spectra were measured at 300 MHz on a Bruker 300 AVANCE III spectrometer with chloroform ($CDCl_3$) or dimethyl sulfoxide (DMSO-d_6) as solvents. UV-Vis absorption spectra were recorded on a Shimadzu 2501 PC spectrophotometer at room temperature. The film for UV-Vis test was fabricated by dropping the polymer solution ($CHCl_3$) onto glass plates and dried before tested. Thermogravimetric analysis (TGA) was performed on a TA Instrument Q500 instrument under a nitrogen atmosphere with a gas-flow rate of 50 mL/min and a heating rate of 10 °C/min. Differential scanning calorimetry (DSC) measurements were carried out on a Mettler Toledo DSC system under a nitrogen atmosphere with a gas-flow rate of 50 mL/min and a heating rate of 20 °C/min. Glass transition temperature was recorded as the temperature at the middle of the thermal transition in the second heating scan. Gel permeation chromatography (GPC) traces of the samples were monitored on an Agilent 1260 GPC-MDS system fitted with differential refractive index (DRI) and Ultraviolet (UV) detectors using THF as the eluent and linear polystyrenes as the molecular weight standards. Cyclic voltammetry (CV) measurements were carried out with a CHI 604E Electrochemical Workstation (CH Instruments, Shanghai Chenhua Instrument Corporation, China) under an argon atmosphere. The polymer film coated on a Pt plate (working electrode) was scanned at 10 mV/s in an anhydrous dichloromethane solution of tetrabutylammonium hexafluorophosphate (*n*-Bu_4NPF_6, 0.1 M), with a Pt wire and platinum gauze as the reference and counter electrodes, respectively. The thickness of the polymer film was measured by a KLA Tencor Alpha-Step Surface Profiler.

Synthesis of monomer and polymer

4,7-Dibromo-*5-(N*-entaphenylmethylene)-6-aminobenzothiadiazole (**6**)

RSC Advances Accepted Manuscript

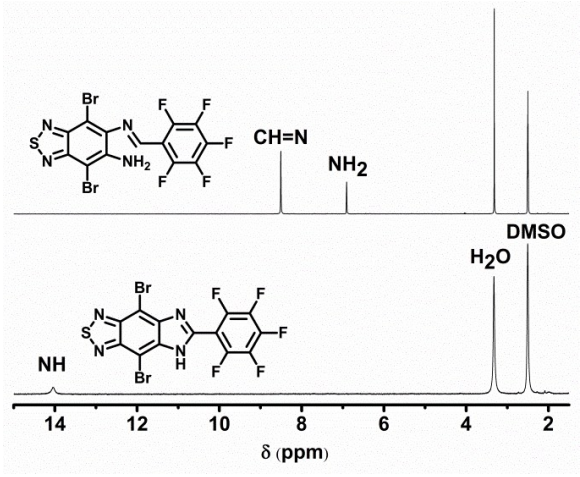

Figure 1. The ^{1}H NMR spectrum of **6** and **M1**

2,3,4,5,6-Pentafluorobenzaldehyde (**5**) (784.2 mg, 4 mmol) and compound **4** (1296 mg, 4 mmol) were thoroughly mixed in DMF (20 mL), and *p*-methylbenzenesulfonic acid (60 mg) was added. the resulted solution was stirred overnight. The reaction mixture was poured into water and extracted with EtOAc (3 ×100 mL), and washed with brine (3 ×100 mL). After dried by $MgSO_4$, the organic solvent was evaporated under reduced pressure. The crude product was purified through column chromatography (eluent: DCM/hexane = 1:4) to yield **6** as a pale solid (1.6065 g, 80 %). ^{1}H NMR (300 MHz, DMSO-d_6): δ (ppm) 8.51 (s, 1H, CH=N), 6.91 (s, 2H, NH_2). ^{19}F NMR (282 MHz, DMSO-d_6): δ (ppm), -145.66 (dd, 2F, J = 25.2 Hz, 8.4 Hz), -153.22 (t, 1F, J = 23.7 Hz), -162.23 (td, 2F, J = 24.9, 11.2 Hz)

4,7-Dibromo-2-(2,3,4,5,6-pentafluorophenyl)-5*H*-imidazo[4,5-*f*]-2,1,3-benzothiadiazole *(***M1***)*.

Compound **5** (502 mg, 1 mmol) was dissolved into DMF (10 mL), and $FeCl_3{\cdot}6H_2O$ (200 mg) was added into the mixture. And the stirred solution was then heated at ca. 80 °C for 3h (monitored by TLC). After the reaction mixture was allowed to cool to room temperature and then added dropwise into a vigorously stirred 0.05 M aq. Na_2CO_3 (100 mL). The reaction mixture was poured into water and extracted with DCM (3 ×50 mL), and washed with brine (3 ×50 mL). After dried by $MgSO_4$, the organic solvent was evaporated under reduced pressure. The crude product was purified through column chromatography (eluent: DCM/hexane = 1:4) to yield **M1** as a brightly yellow solid (460 mg, 92 %). ^{1}H NMR (300 MHz, DMSO-d_6): δ (ppm), 14.02 (s, 1H, NH). ^{19}F NMR (282 MHz, DMSO-d_6): δ (ppm), -138.23 (d, 2F, J = 26.7 Hz), -148.81 (t, 1F, J = 24.3 Hz), -161.03 (t, 2F, J = 24.9Hz).

PIBT-BDT

The equimolecular amounts of **M1** and **M2** (0.15 mmol), and $Pd(PPh_3)_4$ (~1.6 mol%) were dissolved in anhydrous toluene. Argon was bubbled through the solution for 30 min and then the mixture was vigorously stirred at 110 °C under an argon atmosphere for 48 h. After cooling to room temperature, the mixture was poured into methanol. After washed with methanol, oligomers and catalyst residues were removed by hexane through a Soxhlet apparatus for 24 h. Then, the product was extracted by tetrahydrofuran (THF) for another 24 h. The THF extraction was concentrated and the product was precipitated by methanol, and collected by filtration and dried in vacuum overnight. Deeply blue powders (129 mg, yield

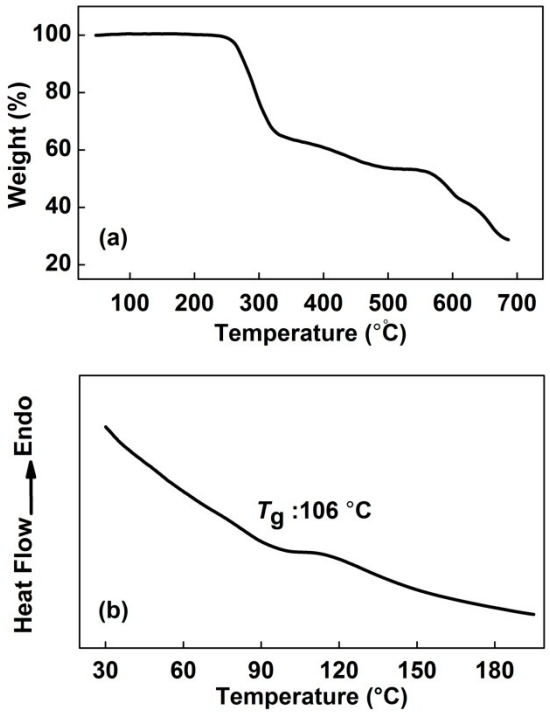

Figure 2. TGA (a) and DSC (b) curves of **PIBT-BDT** under argon atmosphere.

83 %). ^{1}H NMR (300 MHz, $CDCl_3$): δ (ppm): 10.64 (s), 9.66 (s), 9.15-8.69 (m), 7.63-7.36 (m), 7.18 (d), 7.08 (d), 6.90 (s), 6.36 (s), 4.51 (br), 4.22 (s), 1.28 (br), 0.91-0.82 (m).

Fabrication and characterization of memory devices

The ITO glasses were washed with ethanol, isopropanol and acetone sequentially in an ultrasonic bath for 20 min, respectively. A 0.1 mL chlorobenzene solution of the polymer **PIBT-BDT** was spin-coated onto the ITO substrates at a spinning speed of 400 rpm for 12 s and then 2000 rpm for 40 s, followed by a vacuum-drying at 100 °C for 8 h. Before spin-coating, the solution was filtered through polytetrafluoroethylene (PTFE) membrane micro-filters with a pore size of 0.45 μm. The thickness of the polymer film is ~97 nm, as measured by spectroscopic ellipsometer (model M2000DI, Woollam). To construct the Au/**PIBT-BDT**/ITO structures, Au top electrodes with a diameter of 100 μm and thickness of 100 nm were deposited at room temperature by thermal evaporation with a metal shadow mask. The current–voltage (*I*–*V*) characteristics of the Au/**PIBT-BDT**/Pt devices were measured in an ambient atmosphere on Keithley 4200 SCS semiconductor characterization system in voltage sweeping mode. The sweeping step is 0.01 V.

RESULTS AND DISCUSSION

Characterization of polymer structures

The synthetic route for the monomer and polymer is shown in **Scheme 1**. The monomer **M1** was synthesized by the condensation and cyclization of 4,7-dibromo-5,6-diaminobenzothiadiazole **4** and 2,3,4,5,6-pentafluorobenzaldehyde **5**. The intermediate product **6** was obtained by the condensation reaction between compounds **4** and **5** in the presence of *p*-TsOH as a catalyst. Although several other organic acid and hydrochloric acid have been tried as catalysts for this reaction, only *p*-TsOH as a catalyst gave the best

RSC Advances Accepted Manuscript

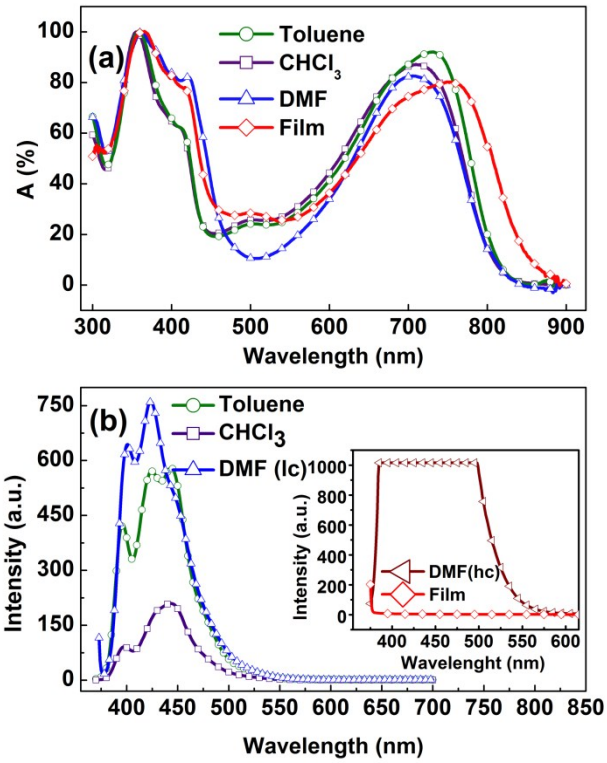

Figure 3. a) UV/Vis absorption spectra of **PIBT-BDT** in solution and as films; b) Photoluminescence spectra of **PIBT-BDT** in solution, and the insets are the PL spectra of polymer in DMF (10^{-5} M) and as films.

result . Note that compound **6** cannot be converted to **M1** without the oxidant agents even heated to 80 °C in the DMF for two days under air. The intermediate product **6** and monomer **M1** were characterized by ^{1}H and ^{19}F NMR spectra. As shown in **Figure 1**, two peaks at 8.51 and 6.91 ppm are observed in the ^{1}H NMR spectrum of 6, which are typical peaks for the proton from imide bonds (CH=N) and amino group with strong electron-withdrawn units. After cyclization, only one peak at 14.02 ppm can be found in the ^{1}H NMR spectrum of the product **M1**. In addition, the ^{19}F NMR results can agree with the chemical structures of **6** and **M1** very well. D-A polymer P1 was synthesized through the Stille coupling polymerization between **M1** and **M2**. The chemical structure of the as-synthesized polymer **PIBT-BDT** can be confirmed by the ^{1}H NMR spectrum. The molecular weight and polydispersity index (PDI) were characterized by GPC with calibration against polystyrene standards and THF as an eluant. The weight-average molecular weight of **PIBT-BDT** is 14 kDa and the polydispersity index is 1.76 by GPC analysis. **PIBT-BDT** exhibits good solubility in common organic solvents, such as DMF, THF, chloroform and chlorobenzene.

Thermal properties

The thermal properties of the as-synthesized polymer **PIBT-BDT** were evaluated by TGA and DSC under nitrogen atmosphere. As shown in **Figure 2**, **PIBT-BDT** was found to have a degradation temperature ($T_{d10\%}$) of 276 °C and a glass transition temperature (T_g) of 106 °C. The results suggest that this polymer is a thermally stable polymer, which can be used in the microelectronics industry.

Optical and electrochemical properties

The UV-vis absorption spectra of the polymer **PIBT-BDT** in solution and thin film state are shown in **Figure 3a**. It can be found that the UV-Vis absorption spectrum of **PIBT-BDT** in $CHCl_3$ shows a maximum absorption peak at ~355 nm with a shoulder peak at ~41[illegible] nm, which can be ascribed to the π–π* transition of the conjugated polymer backbone. A broad bands in the range of 500-800 nm can be observed with a maximum absorption peak at ~712 nm, and this peak is due to the coupling between the n–π* and π–π* transitions of imidazole units, as well as the intramolecular charge-transfer (CT) interaction of **PIBT-BDT** as a dilute solution in chloroform.[47] As expected, both absorption bands of **PIBT-BDT** film are obviously broader than those of **PIBT-BDT** dilute solution. The red shifts of maximum absorption peaks are $\Delta\lambda$=9 nm and $\Delta\lambda$=45 nm, respectively, indicating that the polymer chains are stacked more tightly to be extended π–π stacking between the D and A moieties.[48] As increasing the polarity of the studied solvents, the absorption maxima of π–π* transition show slightly redshifts, whereas these of n–π* and π–π* transitions exhibit significant blue shift, which suggests that the energy barrier of π–π* transition in the polymer mainchain did not change very much by the polarity of solvent, however, the energy barrier of n–π* and π–π* transitions is enlarged by increasing the polarity of the solvents, especially the formation of the hydrogen bonds between solvents and imidazole units.

To further investigate the optical properties of this novel IBT-including polymer, we measured the photoinduced intramolecular charge transfer by the fluorescence spectra in different organic solvents. As shown in **Figure 3b**, the emission spectrum of **PIBT-BDT** in toluene shows strong emission bands at λ_{max}=396, 423 and 444 nm. Interestingly, when the polarity of the organic solvents increased, no obvious change of maximum emission bands was investigated, which suggests the π–π* transition is not affected by the polarity of the solvents very much, and agrees with the UV-Vis results. It is noticeable that the concentration of **PIBT-BDT** in toluene and chloroform solution is ~ 10^{-5} M for the fluorescence testing, but the fluorescence spectrum of a solution of the **PIBT-BDT** in DMF solution with a concentration of 10^{-5} M shows overflow in the range of 384-500 nm (see the **inset of Figure 3b**). The fluorescence spectrum in **Figure 3b** for the **PIBT-BDT** in DMF was recorded after diluting the **PIBT-BDT** in DMF solution to 10^{-7} M, which is still stronger than that in toluene and chloroform solution with a concentration of 10^{-5} M.

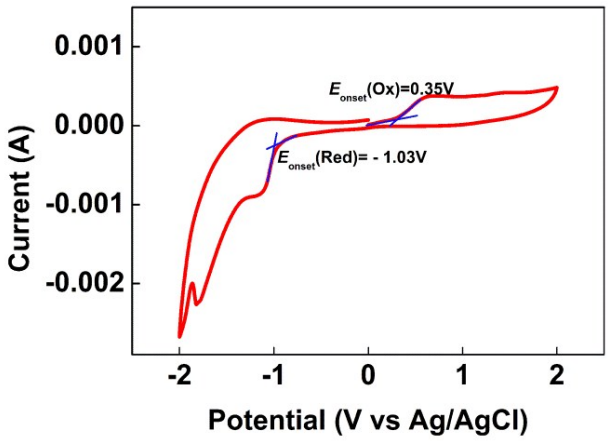

Figure 4. Cyclic voltammograms of **PIBT-BDT** films.

RSC Advances Accepted Manuscript

This journal is © The Royal Society of Chemistry 20xx

Please do not adjust margins

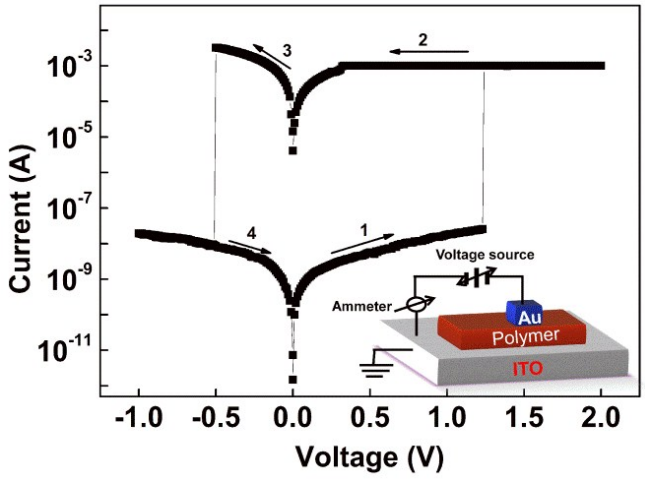

Figure 5. *I–V* characteristics of ITO/ **PIBT-BDT** /Ag memory cells; the inset is a schematic configuration of the Au/PIBT-BDT/ITO devices

Figure 4 shows the cyclic voltammogram of **PIBT-BDT** films with *platinum* plate electrodes using a 0.1 M solution of tetrabutylammonium hexafluorophosphate (n-Bu_4NPF_6) in anhydrous acetonitrile. According to the equation of HOMO/LUMO=−[$E_{ox/red}$−$E_{ox.(ferrocene)}$]−4.8,[49] the HOMO/LUMO values of the samples can be experimentally calculated form the onset of the redox potentials by employing the known reference level for ferrocene, 4.8 eV below the vacuum level. Ferrocene showed an onset oxidation of 0.32 V versus Ag/AgCl in our electrochemical experiments. The first oxidation (E_{ox}) for **PIBT-BDT** is 0.32 V versus Ag/AgCl, whereas the first reduction potential (E_{red}) is -1.03 V versus Ag/AgCl. Therefore, the HOMO of **PIBT-BDT** is -4.83 eV and the LUMO is -3.45 eV.

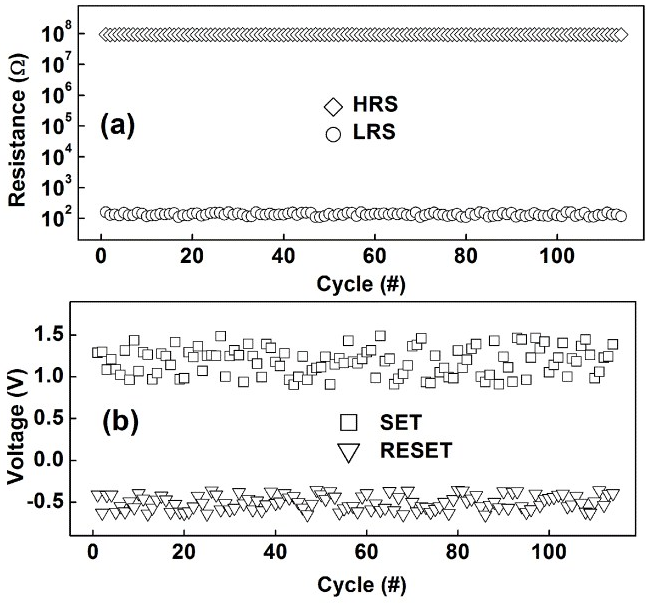

.

Figure 6. The distribution of resistances (a) and programming voltages (b) during the endurance testing.

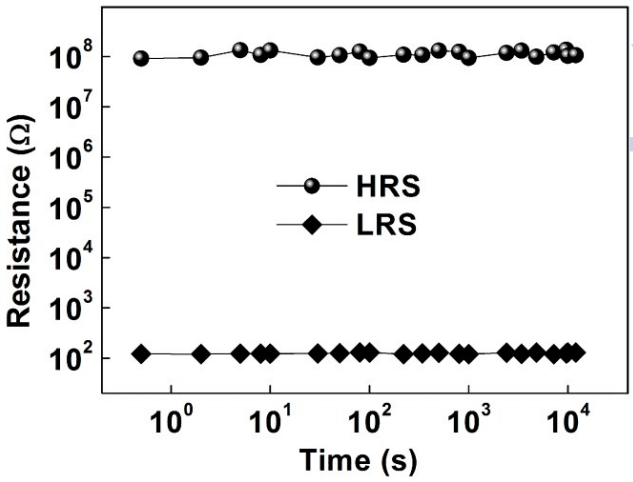

Figure 7. Retention of an Au/**PIBT-BDT**/ITO device.

Memory device characteristics of the polymer.

Au/**PIBT-BDT**/ITO memory device was fabricated and the device structure is shown as the insert of **Figure 5**. The initial resistance of the as-fabricated device is 92.5 MΩ and this state can be named as OFF stated or high resistance stated (HRS). The bottom electrode (ITO) was grounded during the *I-V* sweeping. The typical *I-V* curves of the Au/**PIBT-BDT**/ITO memory device are employed to depict the memory effect process, as shown in **Figure 5**. The current increases gradually and slowly from ~100 pA to ~25 nA when the applying positively-biased voltage sweeps from 0 to 1.23 V. And the current increase abruptly at 1.24 V with further increasing the sweeping voltage, which suggests that the state of this device has switched from a HRS to a low resistance state (LRS or ON state). This transition from OFF state to ON state is defined as a "Write" or "SET" process. Generally, a compliance current (1 mA in this work) is usually required in the "SET" process to prevent a permanent breakdown of the device. During the sweeping voltage from 1.24V to 2V, and 2 V to -0.51 V, the device keeps the ON state (sweeps 2 and 3), indicating the non-volatile characteristic of this memory device. However, the current drops sharply once the voltage exceeds –0.51 V, and this process is generally defined as "Erase" or "RESET" process. This HRS can be kept until the next "Read" process (sweep 4). The ON/OFF ratio of as high as 2.5×10^5 can be achieved, which leads to a low misreading possibility for the memory application

Cyclic switching operations are used to investigate the endurance performance of the Au/**PIBT-BDT**/ITO memory devices. **Figure 6a** exhibits the evolution of the resistance of the two well-resolved states more than 100 cycles. The resistance values are read out at 0.1 V in each sweep. The resistances in the OFF states show no obvious distribution in the endurance testing, whereas the resistances distribution of the ON state can be seen with a slight fluctuation. Generally, the resistance rations are kept more than five orders of magnitude during RS cycles. The evolution of the switching voltages of SET and RESET of the Au/**PIBT-BDT**/ITO devices shows large fluctuation compared to the resistance of the ON and OFF states, as shown in **Figure 6b**. The range of the SET voltages is 0.90~1.49 V, and the range of RESET voltages is -0.65~-0.35 V. In some senses, the endurance measurement suggests that

RSC Advances Accepted Manuscript

the memory effect of this device is controllable, reversible and reproducible.

Figure 7 shows the retention performance of the typical Au/**PIBT-BDT**/ITO device under 0.1 V readout voltage. The readout is nondestructive. The readout measurement was carried out in ambient atmosphere at room temperature. After more than 10^4 s, both the variation of the resistance distribution LRS and HRS states of the device is very small without external electrical power supply, confirming the nonvolatile nature of the device.

The *I-V* curves of the SET process were replotted in a log-log scale, as shown in **Figure 8** to understand the conduction and switching mechanisms of Au/**PIBT-BDT**/ITO devices. The *I-V* curve of the ON state can be satisfactorily fitted with the Ohmic conduction model, however, the fitting of conduction mechanisms of the OFF state faces more difficulty. The fitting results suggest that the charge transport behavior is in good agreement with a classical trap-controlled space charge limited current (SCLC), which consists of three portions: the Ohmic region ($I \propto V$), and the Child's law region ($I \propto V^2$).[6] Therefore, the dominant conduction mechanism of the OFF state is trap-controlled SCLC. The total different conduction behaviors in ON and OFF states suggest that the memory effect may be resulted from the forming/rupturing of the filament, which is composed with the charge transfer complex between the donors and acceptors in the polymer chains.

In the polymer chain, BDT moieties are electron donors and act as nucleophilic sites, whereas the IBT moieties are electron acceptors and act as electrophilic sites. The energy level diagram of Au/polymer/ITO device is shown in **Figure 9**. The energy barrier for the hole injection from the Au to the HOMO of the polymer is estimated to be 0.27 eV, whereas the energy barrier for the electron injection from the ITO to the LUMO of the polymer is 1.35 eV. Therefore, the energy barrier for the hole injection from Au electrodes to the HOMO of the polymer is much lower than that for electron injection from the ITO to the LUMO of the polymer. Thus, the conduction process in the devices is dominated by the hole injection. When applying an increasing positive-biased voltage, holes are injected from the ITO into the HOMO of the polymer gradually. The injected holes are mobilizable by a hopping process among the polymer chains. Charge trapping sites among the polymer chains can lead to a charge accumulation and then a redistribution of the electric field in the polymer layer. When the sweeping voltage increases to the threshold voltage, there will form a conductive path, where almost all the BDT moieties are injected with holes, and then the holes have high mobility to form a conductive filament from the Au electrode to ITO electrode. The current can flow through the filament and sustain the ON state. When the current increases over the compliance current, a large number of charges will flow through the previous formed filament and this process can produce excess heat. In addition, the injected charges into the HOMO of the polymer also increase, and the charges can be trapped in the polymer layer and the interface between the polymer and electrodes. When the applied voltage increases over a certain value (RESET voltage), the injected charges will exceed the capacity of the filament. Excessive current flow will also generate much heat. In the same time, repulsive Coulomb interactions among the trapped charges gathering in the polymer

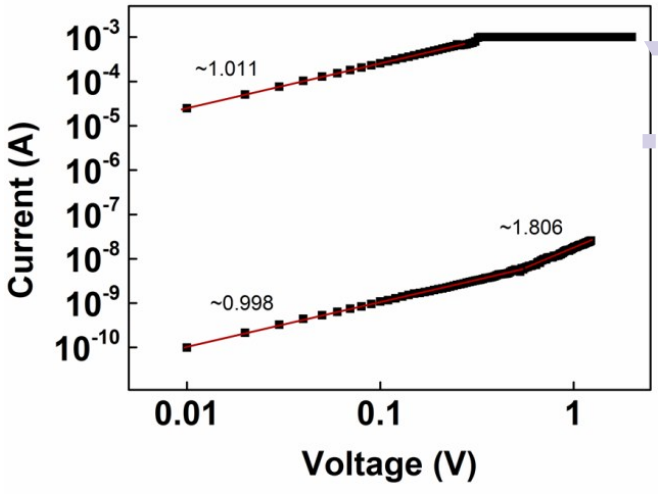

Figure 8. Experimental and fitted *I–V* curves of an Au/**PIBT-BDT**/ITO memory device in both the ON and OFF states during the S process.

layer and the interface may be resulted from the excessive current flow. The heat and Coulomb repulsion will lead to the rupture of the filament formed in the SET process, which will switch the device back to its initial OFF state.

CONCLUSIONS

The D-A polymer **PIBT-BDT** with a novel acceptor, 7-perfluorophenyl-6*H*-[1,2,5]thiadiazole[3,4-*g*]benzoimidazole, was designed and synthesized. The as-synthesized **PIBT-BDT** shows high molecular weight of 14 kDa, strong absorption in the range of 300-800 nm, strong fluorescence in the range of 400-500 nm, and a HOMO/LUMO energy level of -4.83/-3.45 eV. The memory device based on **PIBT-BDT** exhibit large OFF ratio of more than 10^5, good endurance of more than 100 cycles, and long retention of more than 10^4 s. The memory effect is originated from the charge transfer between the strong acceptor (**IBT**) units and the donor **BDT** units. Our results could provide a new horizon to modify the BT unit and design new D-A polymers based on BT units used in organic electronics with excellent device performance.

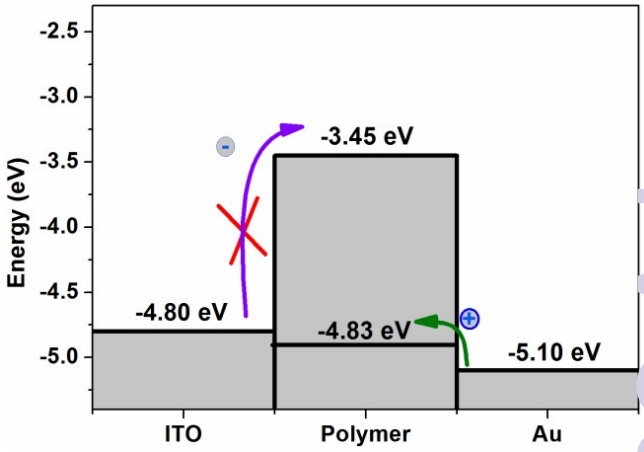

Figure 9. Energy level diagram of Au/**PIBT-BDT**/ITO device.

RSC Advances Accepted Manuscript

This journal is © The Royal Society of Chemistry 20xx

Acknowledgements

The authors thank Mr. Kai Wang for the GPC testing. Q.Z. acknowledges the financial support AcRF Tier 1 (RG 16/12 and R/G 133/14), Tier 2 (ARC 20/12 and ARC 2/13) from MOE, and CREATE program (Nanomaterials for Energy and Water Management) from NRF Singapore.

REFERENCES AND NOTES

1. (a) B. Cho, S. Song, Y. Ji, T.-W. Kim, T. Lee, *Adv. Funct. Mater.* **2011**, 21, 2806-2829. (b) B. Hu, C. Wang, J. Wang, J. Gao, K. Wang, J. Wu, G. Zhang, W. Cheng, B. Venkateswarlu, M. Wang, P. S. Lee, Q. Zhang, *Chem. Sci.* **2014**, 5, 3404 – 3408. (c) J. Li, Q. Zhang, *ACS Appl. Mater. & Interfaces*, 2015, DOI: 10.1021/acsami.5b00113
2. T. Hasegawa, K. Terabe, T. Tsuruoka, M. Aono, *Adv. Mater.* **2012**, 24, 252-267.
3. P. Heremans, G. H. Gelinck, R. Müller, K.-J. Baeg, D.-Y. Kim, Y.-Y. Noh, *Chem. Mater.* **2011**, 23, 341-358.
4. (a) G. Jiang, Y. Song, X. Guo, D. Zhang, D. Zhu, *Adv. Mater.* **2008**, 20, 2888-2898. (b) P.-Y. Gu, F. Zhou, J. Gao, G. Li, C. Wang, Q.-F. Xu, Q. Zhang, J.-M. Lu, *J. Am. Chem. Soc.* **2013**, 135, 14086–14089. (c) G. Li, K. Zheng, C. Wang, K. S. Leck, F. Hu, X. W. Sun, Q. Zhang, *ACS Appl. Mater. & interface* **2013**, *5*, 6458–6462.
5. D.-J. Liaw, K.-L. Wang, Y.-C. Huang, K.-R. Lee, J.-Y. Lai, C.-S. Ha, *Prog. Polym. Sci.* **2012**, 37, 907-974.
6. (a) Q.-D. Ling, D.-J. Liaw, C. Zhu, D. S.-H. Chan, E.-T. Kang, K.-G. Neoh, *Prog. Polym. Sci.* **2008**, 33, 917-978. (b) C. Wang, B. Hu, J. Wang, J. Gao, G. Li, W.-W. Xiong, B. Zou, M. Suzuki, N. Aratani, H. Yamada, F. Huo, P. S. Lee, Q. Zhang, *Chem. Asian J.* **2015**, 10, 116-119. (c) B. Hu, C. Wang, J. Zhang, K. Qian, W. Chen, P. S. Lee, Q. Zhang, *RSC Advances* 2015, **5**, 30542 – 30548.
7. J. C. Scott, L. D. Bozano, *Adv. Mater.* **2007**, 19, 1452-1463.
8. Y. Yang, J. Ouyang, L. Ma, R. J.-H. Tseng, C.-W. Chu, *Adv. Funct. Mater.* **2006**, 16, 1001-1014.
9. D.-H. Kwon, K. M. Kim, J. H. Jang, J. M. Jeon, M. H. Lee, G. H. Kim, X.-S. Li, G.-S. Park, B. Lee, S. Han, M. Kim, C. S. Hwang, *Nat. Nanotechnol.* **2010**, 5, 148-153.
10. M.-J. Lee, C. B. Lee, D. Lee, S. R. Lee, M. Chang, J. H. Hur, Y.-B. Kim, C.-J. Kim, D. H. Seo, S. Seo, U. I. Chung, I.-K. Yoo, K. Kim, *Nat. Mater.* **2011**, 10, 625-630.
11. W. Lu, *Nat. Mater.* **2013**, 12, 93-94.
12. G. I. Meijer, *Science* **2008**, 319, 1625-1626.
13. J. C. Scott, *Science* **2004**, 304, 62-63.
14. R. Waser, M. Aono, *Nat. Mater.* **2007**, 6, 833-840.
15. J. J. Yang, D. B. Strukov, D. R. Stewart, *Nat. Nanotechnol.* **2013**, 8, 13-24.
16. S. Q. Liu, N. J. Wu, A. Ignatiev, *Appl. Phys. Lett.* **2000**, 76, 2749-2751.
17. (a) W. Zhang, C. Wang, G. Liu, J. Wang, Y. Chen, R.-W. Li. *Chem. Commun.* **2014**, 50, 11496-11499. (b) B. Hu, X. Zhu, X. Chen, L. Pan, S. Peng, Y. Wu, J. Shang, G. Liu, Q. Yan, R.-W. Li, *J. Am. Chem. Soc.* **2012**, 134, 17408-17411.
18. (a) P.-Y. Gu, Y. Ma, J.-H. He, G. Long, C. Wang, W. Chen, Y. Liu, Q.-F. Xu, J.-M. Lu, Q. Zhang, *J. Mater. Chem. C.* **2015**, 3, 3167 – 3172. (b) C. Wang, M. Yamashita, B. Hu, Y. Zhou, J. Wang, J. Wu, F. Huo, P. S. Lee, N. Aratani, H. Yamada, Q. Zhang, *Asian J. Org. Chem.* **2015**, 4, 646–651. (c) C. Wang, J. Wang, P. Li, J. Gao, S. Y. Tan, W. Xiong, B. Hu, P. S. Lee, Y. Zhao, Q. Zhang, *Chem Asian J.* **2014**, 9, 779-783. (d) P.-Y. Gu, J. Gao, C.-J. Lu, C. Wang, G. Li, F. Zhou, Q.-F. Xu, J.-M. Lu, Q. Zhang, *Mater. Horizons*, **2014**, 1, 446-451.
19. W. Zhang, C. Wang, G. Liu, X. Zhu, X. Chen, L. Pan, H. Tan, W. Xue, Z. Ji, J. Wang, Y. Chen, R.-W. Li, *Chem. Commun.* **2014**, 50, 11856-11858.
20. C. Wang, G. Liu, Y. Chen, S. Liu, Q. Chen, R. Li, B. Zhang, *ChemPlusChem* **2014**, 79, 1263-1270.
21. J. Yao, L. Zhong, D. Natelson, J. M. Tour, *Sci. Rep.* **2012**, 2, 242.
22. B. Hu, F. Zhuge, X. Zhu, S. Peng, X. Chen, L. Pan, Q. Yan, R.-W. Li, *J. Mater. Chem.* **2012**, 22, 520-526.
23. B. Hu, R. Quhe, C. Chen, F. Zhuge, X. Zhu, S. Peng, X. Chen, L. Pan, Y. Wu, W. Zheng, Q. Yan, J. Lu, R.-W. Li, *J. Mater. Chem.* **2012**, 22, 16422-16430.
24. B. Zhang, G. Liu, Y. Chen, C. Wang, K.-G. Neoh, T. Bai, E.-T. Kang, *ChemPlusChem* **2012**, 77, 74-81.
25. X.-D. Zhuang, Y. Chen, B.-X. Li, D.-G. Ma, B. Zhang, Y. Li, *Chem. Mater.* **2010**, 22, 4455-4461.
26. X.-D. Zhuang, Y. Chen, G. Liu, P.-P. Li, C.-X. Zhu, E.-T. Kang, K.-G. Noeh, B. Zhang, J.-H. Zhu, Y.-X. Li, *Adv. Mater.* **2010**, 22, 1731-1735.
27. A. Klamchuen, H. Tanaka, D. Tanaka, H. Toyama, G. Meng, S. Rahong, K. Nagashima, M. Kanai, T. Yanagida, T. Kawai, T. Ogawa. *Adv. Mater.* **2013**, 25, 5893-5897.
28. X. D. Zhuang, Y. Chen, G. Liu, B. Zhang, K. G. Neoh, E. T. Kang, C. X. Zhu, Y. X. Li, L. J. Niu, *Adv. Funct. Mater.* **2010**, 20, 2916-2922.
29. S.-J. Choi, G.-S. Park, K.-H. Kim, S. Cho, W.-Y. Yang, X.-S. Li, J.-Moon, K.-J. Lee, K. Kim, *Adv. Mater.* **2011**, 23, 3272-3277.
30. S. C. Chae, J. S. Lee, S. Kim, S. B. Lee, S. H. Chang, C. Liu, Kahng, H. Shin, D.-W. Kim, C. U. Jung, S. Seo, M.-J. Lee, T. W. Noh, *Adv. Mater.* **2008**, 20, 1154-1159.
31. G. Liu, Q.-D. Ling, E. Y. H. Teo, C.-X. Zhu, D. S.-H. Chan, K.-G. Neoh, E.-T. Kang, *ACS Nano* **2009**, 3, 1929-1937.
32. Y.-K. Fang, C.-L. Liu, C. Li, C.-J. Lin, R. Mezzenga, W.-C. Chen, *Adv. Funct. Mater.* **2010**, 20, 3012-3024.
33. B. Hu, C. Wang, J. Wang, J. Gao, K. Wang, J. Wu, G. Zhang, W. Cheng, B. Venkateswarlu, M. Wang, P. S. Lee, Q. Zhang, *Chem. Sci.* **2014**, 5, 3404-3408.
34. H.-H. Chang, C.-E. Tsai, Y.-Y. Lai, W.-W. Liang, S.-L. Hsu, C.-S. Hsu, Y.-J. Cheng, *Macromolecules* **2013**, 46, 7715-7726.
35. N. Wang, Z. Chen, W. Wei, Z. Jiang, *J. Am. Chem. Soc.* **2013**, 135, 17060-17068.
36. (a) K. Yao, L. Chen, X. Chen, Y. Chen, *Chem. Mater.* **2013**, 25, 897-904. (b) B. Hu, M. Li, W. Chen, X. Wan, Y. Chen, Q. Zhang, *RSC Advances,* **2015**, 5, 50137 - 50145
37. W. Li, A. Furlan, K. H. Hendriks, M. M. Wienk, R. A. J. Janssen, *J. Am. Chem. Soc.* **2013**, 135, 5529-5532.
38. T. Ameri, P. Khoram, J. Min, C. J. Brabec, *Adv. Mater.* **2013**, 25, 4245-4266.
39. G.-Y. Chen, S.-C. Lan, P.-Y. Lin, C.-W. Chu, K.-H. Wei, *J. Polym. Sci. Part A: Polym. Chem.* **2010**, 48, 4456-4464.
40. V. Percec, G. Johansson, G. Ungar, J. Zhou, *J. Am. Chem. Soc.* **1996**, 118, 9855-9866.
41. R. Souzy, B. Ameduri, B. Boutevin, *Prog. Polym. Sci.* **2004**, 29, 75-106.
42. A. Tressaud, E. Durand, C. Labrugère, A. P. Kharitonov, L. N. Kharitonova, *J. Fluorine Chem.* **2007**, 128, 378-391.
43. M. L. Tang, Z. Bao, *Chem. Mater.* **2011**, 23, 446-455.
44. X. X. Sun, X. X. Zhuang, Y. L. Ren, *Adv. Compos. Mater.* **2012**, 482-484, 1221-1224.
45. Y. Dong, W. Cai, M. Wang, Q. Li, L. Ying, F. Huang, Y. Cao, *Org. Electron.* **2013**, 14, 2459-2467.
46. Y. Koizumi, M. Ide, A. Saeki, C. Vijayakumar, B. Balan, Y. Kawamoto, S. Seki, *Polym. Chem.* **2013**, 4, 484-494.
47. M. Zhang, H. N. Tsao, W. Pisula, C. Yang, A. K. Mishra, K. Müllen. *J. Am. Chem. Soc.* **2007**, 129, 3472-3473.
48. W. Zhang, J. Li, B. Zhang, J. Qin. *Macromol. Rapid Comm.* **2008**, 29, 1603-1608.
49. Y. Chen, M. E. Ei-Khouly, M. Sasaki, Y. Araki, O. Ito. *Org. Lett.* **2005**, 7, 1613-1616.

RSC Advances Accepted Manuscript

Journal Name

ARTICLE

TOC page

Novel Organic Memory Effect from Novel Donor-Acceptor Polymers based on 7-Perfluorophenyl-6*H*-[1,2,5]thiadiazole[3,4-g]benzoimidazole

Benlin Hu, Chengyuan Wang, Jing Zhang, Kai Qian, Pooi See Lee, Qichun Zhang

A novel D-A polymer is designed for resistance memory devices with large OFF ratio, good endurance and long retention time.

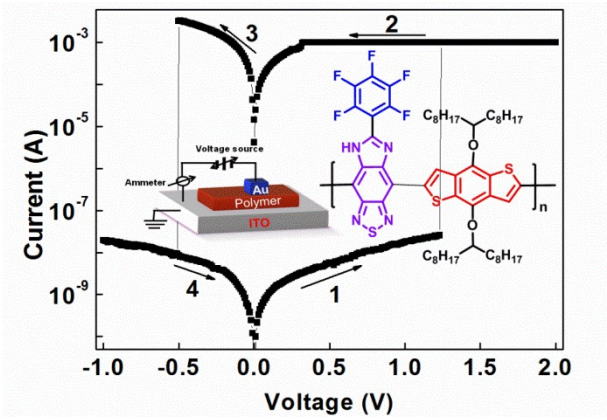

RSC Advances Accepted Manuscript